Journal of Controlled Release 331 (2021) 309–320

Contents lists available at ScienceDirect

Journal of Controlled Release

journal homepage: www.elsevier.com/locate/jconrel

Liposome induction of CD8$^+$ T cell responses depends on CD169$^+$ macrophages and Batf3-dependent dendritic cells and is enhanced by GM3 inclusion

J. Grabowska [a], A.J. Affandi [a], D. van Dinther [a], M.K. Nijen Twilhaar [a], K. Olesek [a], L. Hoogterp [a], M. Ambrosini [a], D.A.M. Heijnen [a], L. Klaase [a], A. Hidalgo [b], K. Asano [c], P.R. Crocker [d], G. Storm [e,f,g], Y. van Kooyk [a], J.M.M. den Haan [a,*]

[a] Department of Molecular Cell Biology and Immunology, Amsterdam University Medical Center, Cancer Center Amsterdam, Amsterdam Infection and Immunity Institute, Vrije Universiteit Amsterdam, Amsterdam, Netherlands
[b] Area of Cell and Developmental Biology, Centro Nacional de Investigaciones Cardiovasculares Carlos III, Madrid, Spain
[c] Laboratory of Immune Regulation, School of Life Science, Tokyo University of Pharmacy and Life Sciences, Tokyo 192-0392, Japan
[d] Division of Cell Signalling and Immunology, School of Life Sciences, University of Dundee, Dundee, UK
[e] Department of Pharmaceutics, Faculty of Science, Utrecht University, Universiteitsweg 99, 3584, CG, Utrecht, the Netherlands
[f] Department of Biomaterials, Science and Technology, Faculty of Science and Technology, University of Twente, Enschede, the Netherlands
[g] Department of Surgery, Yong Loo Lin School of Medicine, National University of Singapore, 117597, Singapore

ARTICLE INFO

Keywords:
Liposomes
CD169
Siglec-1
Macrophage
Dendritic cell
T cell response

ABSTRACT

Cancer vaccines aim to efficiently prime cytotoxic CD8$^+$ T cell responses which can be achieved by vaccine targeting to dendritic cells. CD169$^+$ macrophages have been shown to transfer antigen to dendritic cells and could act as an alternative target for cancer vaccines. Here, we evaluated liposomes containing the CD169/Siglec-1 binding ligand, ganglioside GM3, and the non-binding ligand, ganglioside GM1, for their capacity to target antigens to CD169$^+$ macrophages and to induce immune responses. CD169$^+$ macrophages demonstrated specific uptake of GM3 liposomes *in vitro* and *in vivo* that was dependent on a functional CD169 receptor. Robust antigen-specific CD8$^+$ and CD4$^+$ T and B cell responses were observed upon intravenous administration of GM3 liposomes containing the model antigen ovalbumin in the presence of adjuvant. Immunization of B16-OVA tumor bearing mice with all liposomes resulted in delayed tumor growth and improved survival. The absence of CD169$^+$ macrophages, functional CD169 molecules, and cross-presenting Batf3-dependent dendritic cells (cDC1s) significantly impaired CD8$^+$ T cell responses, while B cell responses were less affected. In conclusion, we demonstrate that inclusion of GM3 in liposomes enhance immune responses and that splenic CD169$^+$ macrophages and cDC1s are required for induction of CD8$^+$ T cell immunity after liposomal vaccination.

1. Introduction

Although checkpoint inhibitors have emerged as a powerful immunotherapy for cancer patients, the majority of cancer patients still do not benefit from this treatment regimen [1–3]. A combination of immunotherapy with checkpoint inhibitors and a cancer vaccination strategy is expected to act synergistically *via* activation of immune responses [4–7].

A variety of vaccine strategies have been explored to induce anti-cancer immune responses [8]. To stimulate cytotoxic CD8$^+$ T cells, vaccine-delivered tumor antigens need to be presented by cross-presenting DCs (cDC1) in an effective manner. Unfortunately, this process is often suboptimal, exposing a bottleneck in cancer vaccine development [9,10]. Our previous research has revealed that cross-presenting cDC1 collaborate with CD169$^+$ (Siglec-1/Sialoadhesin) macrophages in the spleen to induce adaptive immune responses. We and others have observed that antigens targeted to CD169$^+$ macrophages were efficiently transferred to cDC1 and elicited potent CD8$^+$ T cell responses that inhibited tumor outgrowth [11–14]. In addition, the direct induction of anti-tumor T cell responses by CD169$^+$ macrophages has also been proposed [14,15]. These observations suggest that vaccines that are efficiently taken up by CD169$^+$ macrophages may optimally stimulate anti-tumor immunity.

* Corresponding author at: Department of Molecular Cell Biology and Immunology, Amsterdam UMC, P.O. Box 7057, 1007 MB Amsterdam, the Netherlands.
E-mail address: j.denhaan@amsterdamumc.nl (J.M.M. den Haan).

https://doi.org/10.1016/j.jconrel.2021.01.029
Received 23 November 2020; Received in revised form 16 January 2021; Accepted 19 January 2021
Available online 22 January 2021

The primary function of CD169$^+$ macrophages located in the lymph nodes and spleen is to scavenge pathogens and endogenous sialic acid-containing particles from the lymph fluid and blood, respectively [16–18]. The CD169 receptor binds sialylated glycoproteins and glycolipids present on the pathogen surface [19]. Binding of HIV virions to human CD169 is mediated *via* a host-derived sialylated glycosphingolipid, the ganglioside GM3 [20–22]. Previously, GM3 was identified as a high affinity binder to mouse CD169 and GM1 ganglioside as a non-binder [23–25].

Liposomes are an attractive antigen delivery system and have already been verified as an effective vaccination platform [26–28]. The aim of the present study was to selectively deliver antigen to splenic CD169$^+$ macrophages using i.v. administered liposomes containing GM3 as targeting molecule. We have evaluated the uptake, the immunogenic capacity, and anti-tumor reactivity of control, GM3 and GM1 liposomes containing ovalbumin (OVA) protein as an antigen encapsulated in the liposome core. In addition, we performed mechanistic studies, which revealed important roles of CD169$^+$ macrophages, the CD169 receptor and Batf3-dependent cDC1s in the activation of CD8$^+$ T cell responses after vaccination with these liposomes. Our findings shed light on the mechanisms responsible for the immunogenicity of liposomes and aid further optimization of liposomal cancer vaccines.

2. Materials and methods

2.1. Mice

C57Bl6/J and Batf3KO mice obtained from Charles River or the Jackson Laboratory. W2QR97A mutant animals, also referred to in the text as CD169 mutant animals, harboring two amino acid substitutions (Trp2 to Gln, Arg97 to Ala) in the CD169 receptor were generated at University of Dundee (Dundee, Scotland) [29]. CD169-DTR mice were generated by Dr. M. Tanaka from the Tokyo University of Pharmacy and Life Sciences (Tokyo, Japan) [30,31]. All mouse lines were bred were bred at the animal facility of Amsterdam UMC (Amsterdam, The Netherlands). Mice used in the study predominantly females between 8 and 12 weeks of age. For CD169-DTR experiments, heterozygous mice were administered or not (control) with diphtheria toxin (DT) two days prior to immunization. All animals were kept under specific pathogen-free conditions and used in accordance with local animal experimentation guidelines.

2.2. Liposome preparation and characterization

Liposomes were prepared from a mixture of phospholipids and cholesterol utilizing the film extrusion method as described previously [76]. In brief, during the first step of the preparation, egg phosphatidylcholine (EPC)-35 (Lipoid), egg phosphatidylglycerol (EPG)-Na (Lipoid) and Cholesterol (Sigma-Aldrich) were mixed at a molar ratio of 3.8:1:2.5, combined with 0,1 mol% of the lipophilic fluorescent tracer DiD (1′-dioctadecyl-3,3,3′,3′-tetramethyl indodicarbocyanine, Life Technologies) and where indicated with 3 mol% GM3 ganglioside (monosialodihexosylganglioside) (Avanti Polar Lipids) or 3 mol% GM1 ganglioside (monosialotetrahexosylganglioside) (Avanti Polar Lipids). A solution of 4 mg/ml or 1 mg/ml Ovalbumin (OVA, Calbiochem) was encapsulated into liposomes during the hydration step, as described previously (Unger et al., 2012). In order to obtain liposomes of approximately 200 nm, hydrated preparations were sequentially extruded through stacked 400 and 200 nm polycarbonate filters using high-pressure extrusion device. Next, to remove non-encapsulated gangliosides and OVA, the liposomal solutions were pelleted in an ultracentrifuge (Beckman) for 60 min at 200,000 *g*. In between the centrifugation steps, after removal of the supernatant, the pellet was resuspended in fresh Hepes buffer pH 7.5 containing 50 U/ml penicillin and 50 μg/ml streptomycin (Lonza). Obtained in the following way liposomes were exposed to quality control analysis where size, polydispersity index and zeta potential were determined using dynamic light scattering (DLS) (Zetasizer Nano ZSP) (Malvern Instruments).

2.3. Sandwich ELISA for OVA content determination

OVA encapsulation efficiency was determined in an sandwich ELISA. MaxiSorp ELISA plates (NUNC, Denmark) were coated with 1 μg/ml purified anti-chicken Ovalbumin (OVA, Biolegend) in coating buffer (pH 9.2) o/n at 4 °C. The following morning the plates were washed with PBS containing 0.05% Tween20 and blocked with 1% BSA/PBS for 1 h at RT. Diluted in PBS liposomes and standard OVA (Sigma), were treated with 0.1% Triton-X for 1 h at RT on a shaking plate. Washed with 0.05% Tween20/PBS plates were incubated with serial dilutions of Triton-X-treated liposomes and OVA standard for 1 h at RT on a shaking plate. Next, the plates were washed with 0.05% Tween20/PBS and incubated with polyclonal rabbit anti-OVA Ig for 1 h at RT on a shaking plate. After washing, goat-anti-rabbit IgG-HRP (Thermofisher) was added for 30 min at RT on a shaking plate and the plates were washed with 0.05% Tween20/PBS. To develop the reaction, 100 μg/ml of TMB (Sigma-Aldrich) was used as a substrate. The absorbance was measured at 450 nm using microplate absorbance spectrophotometer (Biorad). The amount of encapsulated OVA was calculated as 13–15 μg/ml liposomes, reaching loading efficiency of approximately 0.2%.

2.4. CD169 Fc and PNA ELISA

MaxiSorp ELISA plates (NUNC, Denmark) were coated with 25 μmol liposomes dissolved in 100% ethanol and left to air dry overnight. The following morning the plates were blocked with 1% BSA/PBS (Fraction V, Fatty acid free, Calbiochem) and washed with PBS. Next, for CD169-Fc ELISA the plates were incubated with 2 μg/ml mouse CD169 Fc WT or R97A mutant conjugate (mouse CD169 fused to Fc fragment of human IgG1, in house-made) for 1 h at RT and directly after PO goat anti-human IgG-Fc (Thermo Fisher Scientific) in 1% BSA/PBS was added for 30 min at RT. For PNA ELISA, the plates were incubated with 5 μg/ml PNA-biotin (Vector laboratories) for 1 h at RT and directly after streptavidin-HRP (Invitrogen) in 1% BSA/PBS was added for 30 min at RT. After the incubation, the plates were washed with PBS. To develop the reaction, 100 μg/ml of TMB (Sigma-Aldrich) was used as a substrate. The absorbance was measured at 450 nm using microplate absorbance spectrophotometer (Biorad).

2.5. Liposome uptake by CD169-expressing CHO cells

CD169-expressing WT and R97A mutant Chinese hamster ovary cells (CHO cells) (gift from Prof. Paul R. Crocker, Dundee, Scotland) were maintained in RPMI-1640 (Gibco, Life Technologies) supplemented with 10% FCS (Biowest), 50 U/ml penicillin, 50 μg/ml streptomycin, 2 mM L-glutamine (all Lonza) and 1 mg/ml G418 (Santa Cruz). Following harvesting, the cells were seeded in 96-well plates at 1×10^5 cells/well. Prior to liposome incubation, CHO WT cells were incubated with 10 μg/ml of blocking anti-CD169 Ab (clone SER-4, in-house made) for 20 min at 4 °C. Next, 0.1 mmol liposomes in HBSS containing 0.5% BSA were added to the cells for 60 min at 37 °C. Following two washing steps, the cells were stained with Fixable Viability Dye eFlour 780 (eBioscience) and measured using Fortessa (BD Biosciences) FACS analyser. Flow cytometry analysis was performed using FlowJo software (Tree Star).

2.6. Spleen digestion

Spleens of WT and W2QR97A mutant mice were digested as previously described [12]. Briefly, mechanistically dissociated spleens were digested using a mixture of 4 mg/ml Lidocaine, 2 WU/ml Liberase TL (Roche, Germany) and 50 μg/ml DNase I (Roche, Germany) for 15 min at 37 °C with continuous stirring. After adding RPMI-1640 (Gibco, Life Technologies) supplemented with 10% heat-inactivated FCS (Biowest),

10 mmol EDTA, 20 mmol HEPES and 50 μM 2-mercaptoethanol, splenocytes were incubated for additional 10 min at 4 °C with continuous stirring. Next, red blood cells were lysed using ammonium-chloride-potassium (ACK) lysis buffer and splenocytes were filtered through 70–100 μm filter.

2.7. Liposome binding to splenocytes

For *in vivo* liposome binding assay, mice were immunized i.v. with 93 nmol of control-OVA or GM3 and GM1 ganglioside-containing OVA liposomes in presence of 25 μg of poly(I:C) and 25 μg anti-CD40 Ab (clone 1C10). Two hours after liposome administration the mice were sacrificed and the spleens were collected. Digested splenocytes were seeded in 96-well plates at 3×10^6 cells/well for flow cytometry. For *in vitro* liposome binding assay, digested splenocytes were seeded in 96 wells at 3×10^6 cells/well and incubated 10 μg/ml of blocking anti-CD169 Ab (clone SER-4, in-house made) for 20 min at 4 °C. Subsequently, 0.1 mmol liposomes in HBSS/0.5% BSA were added to the cells for 60 min 4 °C or 37 °C. Following two washing steps with PBS/0.5% BSA, the cells were stained for flow cytometry.

2.8. Immunofluorescence microscopy

To obtain tissue sections for immunofluorescence microscopy, spleen blocks cryopreserved in liquid nitrogen were cut at 5–6 μm thickness using CryoStar NX70 (Thermo Scientific). After blocking of unspecific binding with 10% normal goat serum in PBS for 20 min at RT, tissue sections were stained with anti-CD169-Alexa Fluor 488 (clone SER-4, in-house made) and anti-B220-biotin (clone RA3-6B2, BD Biosciences) for 45 min at RT. Next, the slides were incubated with a Alexa Fluor 555-conjugated streptavidin for 30 min at RT, followed by incubation with DAPI for 10 min at RT. Mounted with a coverslip slides were analyzed with Leica DM6000 using 10× objective. LAS AF software was used for image acquisition and processing. Exposure time for DiD signal was adjusted using tissue sections of uninjected mice, while for the adjustment of the exposure times for other channels unstained tissue sections were used. The following filter cubes/fluorochromes combinations were used: A4/DAPI, L5/Alexa Fluor 488, N3/Alexa Fluor 555 and Y5/DiD.

2.9. Evaluation of antigen-specific T cell and B cell responses

To investigate antigen-specific T cell and B cell responses, WT, CD169-DTR, CD169 mutant mice and Batf3KO mice were injected i.v. with 93 nmol and 200 nmol respectively of control-OVA or ganglioside-containing OVA liposomes in presence of 25 μg of poly(I:C) and 25 μg anti-CD40 Ab (clone 1C10). For immunization experiments performed in CD169-DTR model, the mice were administered with 40 ng/g of DT i.v. 2 days pre-immunization with liposomes. On day 7 p.i., splenocytes were collected as previously described [12]. Digested splenocytes were seeded in 96-well plates at 3×10^6 cells/well and used for direct tetramer staining, direct germinal center B cell staining and intracellular IFNγ staining following re-challenge with OVA peptide *in vitro*. Identification of OVA-specific $CD8^+$ T cell and B cell responses was directly performed by flow cytometry. For determination of $CD8^+$ and $CD4^+$ T cell responses following re-challenge with cognate peptide, the cells were incubated with MHC class I restricted OVA 257–264 peptide (0.1 μg/ml) in presence of GolgioPlug (BD Biosciences) for 5 h or with MHC class II restricted OVA 262–276 peptide (100 μg/ml) for 23 h with last 5 h also in presence of GolgiPlug (BD Biosciences). Next, flow cytometry staining was performed.

2.10. Determination of anti-OVA titer in the serum

To determine the anti-OVA Ig titer in the serum of liposome-immunized mice, serum was obtained by centrifugation of blood collected on day 7 p.i.. MaxiSorp ELISA plates (NUNC, Denmark) were coated with 5 μg/ml OVA (Sigma-Aldrich) in sodium phosphate buffer (Na_2HPO_4, NaH_2PO_4 and MiliQ, pH 6.5) o/n at 4 °C. The following morning the plates were washed with 0.05% Tween20/PBS and blocked with 1% BSA/PBS for 1 h at RT. After washing, serial dilutions of serum in 1% BSA/PBS were incubated for 2 h at RT. Next, rabbit anti-mouse Ig-HRP (Dako) in 1% BSA/PBS was added to the washed plates for 1 h at RT. To develop the reaction, 100 μg/ml of TMB (Sigma-Aldrich) was used as a substrate. The absorbance was measured at 450 nm using microplate absorbance spectrophotometer (Biorad). An average + 3× SD of OD values measured in blank wells without serum OD value was assigned as a cut-off value. Antibody titers were determined as dilutions with corresponding OD values higher than the cut-off.

2.11. Flow cytometry

Cells were first incubated with 10 μg/ml of anti-CD16/32 (clone 2.4G2, in-house made) for 15 min at 4 °C to block unspecific Fc receptor binding and subsequently stained with an appropriate surface antibody panel containing a Fixable Viability Dye eFlour 780 (eBioscience) in PBS/0.5% BSA for 30 min at 4 °C. To identify specific immune cell populations in the spleen, the cells were stained with antibodies or fluorescent reagents provided in Table 1. For direct identification of OVA-specific $CD8^+$ T cells using H-$2K^b$/SIINFEKL tetramers, cells were stained at 37 °C for 60 min. To evaluate OVA-specific B cell responses, cells were stained at 4 °C for 30 min. For intracellular IFNγ staining, first surface staining was performed. The cells were fixed with 2% paraformaldehyde (Electron microscopy science) for 20 min at 4 °C, permeabilized with 0.5% Saponin solution and stained for intracellular cytokine. After washing the cells were measured using Fortessa (BD) FACS analyser. Flow cytometry analysis was performed using FlowJo software (Tree Star).

2.12. Tumor challenge and therapeutic vaccination

Melanoma B16-OVA cells (kind gift from Prof. T.N. Schumacher, Netherlands Cancer Institute) [32] were maintained in RPMI-1640 (Gibco, Life Technologies) supplemented with 10% FCS (Biowest), 50 U/ml penicillin and 50 μg/ml streptomycin, 2 mM L-glutamine (all Lonza) and passaged at 70% confluency. Eight weeks old C57Bl6/J animals were injected subcutaneously (s.c.) in the flank with 3×10^5 B16-OVA cells in 100 μl HBSS. Tumor dimensions were measured by digital caliper 3× per week and used to calculate tumor volume with modified ellipsoid formula: L x W^2 x PI/6 [33]. Mice were sacrificed when tumor reached humane end point (HEP), thus size 800–1000 mm^3. On day 9, when tumors were palpable (tumor size range 0,5–30 mm^3), the mice were randomized into treatment groups (average size of 12,5 mm^3) and immunized i.v. with 93 nmoles of OVA-containing liposomes in presence of 25 μg of poly(I:C) and 25 μg anti-CD40 Ab (clone 1C10). Seven days after vaccination, blood was collected from the cheek to determine the expansion of antigen-specific $CD8^+$ T cells. Obtained blood cells were centrifuged, exposed to ACK lysis buffer to remove red blood cells and stained with $CD8^+$ T cell tetramer antibody mixture.

2.13. Statistical analysis

Statistical significance was determined in GraphPad Prism software using one-way ANOVA test with Bonferroni's multiple comparison test or two-way ANOVA test with Tukey's multiple comparison test ($*p < 0.05$, $**p < 0.01$). All values are expressed as ±SEM with individual mice showed.

3. Results

3.1. GM3 liposomes specifically bind to CD169 in vitro

We generated small anionic liposomes containing ovalbumin protein

Table 1
List of antibodies/fluorescent reagents used for flow cytometry.

Antigen/reagent	Fluorochrome	Clone	Company	Panel
CD169	Alexa Fluor 488	SER-4	in-house made	Macrophage/DC/B cell/liposome
B220	Alexa Fluor 405	6B2	in-house made	
F4/80	PE-CF594	T45–2342	BD Biosciences	
CD8a	PE-Cy7	53–6.7	BD Biosciences	
CD11c	BV650	HL3	BD Biosciences	
I-A/I-E	PE	M5/114.15.2	eBioscience	
I-A/I-E	Alexa Fluor 405	M5/114	in-house made	
CD11b	PE-Cy7	M1/70	eBioscience	NK cell/T cell/monocyte/liposome
Ly6C/Gr-1	eFluor 450	RGG6-8C5	eBioscience	
CD3	FITC	145-2C11	eBioscience	
NK 1.1	BV650	PK136	BD Biosciences	
CD8a	APC	53–6.7	BD Biosciences	$CD8^+$ T cell tetramer staining
CD44	FITC	KM81	Immunotools	
H-$2K^b$/SIINFEKL	PE tetramer	N/A	LUMC, Leiden	
B220	BV510	RA3-6B2	Biolegend	Germinal B cell staining
CD38	PE	90/CD38	BD Biosciences	
GL7	PE-Cy7	GL-7	Biolegend	
OVA	Alexa Fluor 488	N/A	Invitrogen	
CD11a	FITC	M17/4	eBioscience	*Re*-stim intracellular IFNγ staining
CD8a	PE-Cy7	53–6.7	BD Biosciences	
CD4	PE	GK1.5	eBioscience	
IFNγ	APC	XMG1.2	eBioscience	

(OVA) in the aqueous core and carrying 3 mol% of ganglioside molecules GM3 or GM1 and 0.1 mol% of the lipophilic DiD dye in the bilayer (Fig. 1A-C). The inclusion of GM3 or GM1 did not affect the zeta potential, size and the polydispersity index of the liposomes compared to control liposomes. Ganglioside GM3 with a terminally oriented α2,3-linked sialic acid group was included as a primary CD169 targeting ligand since it was previously shown to mediate specific recognition of virus particles by CD169 [34]. Contrary to ganglioside GM3, ganglioside GM1 contains an internally positioned sialic acid residue resulting in a weak CD169 interaction, and therefore served as a negative control, next to the non-targeting control liposomes [25].

To confirm the incorporation of gangliosides into the liposomes and subsequently assess their binding specificity to CD169, we performed an ELISA assay using recombinant CD169 Fc WT and CD169 Fc mutant protein, which harbors mutations in the ligand binding part of the receptor (R97A) rendering it incapable of sialic acid recognition [29]. As

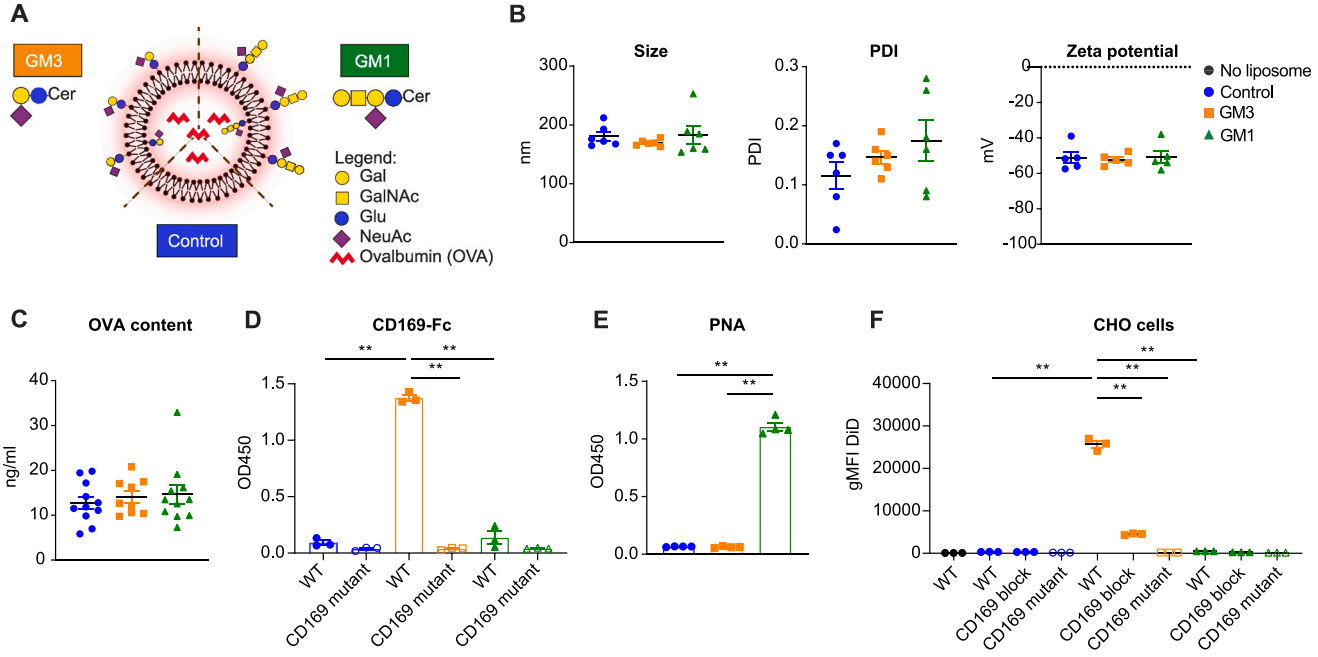

Fig. 1. Characterization of the liposomal formulations. A. Schematic representation of control and ganglioside liposomes composed of phospholipid bilayer (cholesterol not shown) incorporated with ganglioside GM3 and GM1 structures and lipophilic DiD tracer (red glow) encapsulating ovalbumin protein (OVA) in the aqueous core. Gal, galactose; Glu, glucose; GalNAc, N-Acetylgalactosamine; NeuAc, sialic acid; GM3, ganglioside GM3; GM1, ganglioside GM1. B. Determination of particle size, PDI (polydispersity index) and zeta potential of prepared liposomal formulations. The data are from five batches of liposomes used in the study. C. Determination of the amount of encapsulated OVA in batches prepared with 1 mg/ml OVA, expressed in ng per ml of liposomal solution. The data are of minimum four batches, from three experiments. D-E Binding of liposomes to WT and mutant CD169 Fc conjugates (D) and PNA (E) determined by ELISA. The data are mean of triplicates from three (D) and four (E) different batches of liposomes. PNA, peanut agglutinin. F. Uptake of liposomes by CD169-expressing CHO WT and CHO mutant cells illustrated by DiD geometric mean fluorescence intensity (gMFI). The data are from one experiment representative of two experiments. Error bars indicate mean ± SEM. $*p < 0.05$, $**p < 0.01$ (one-way ANOVA with Bonferroni's multiple comparison test (A-C,F) and two-way ANOVA with Tukey's multiple comparison test (D-E)). (For interpretation of the references to colour in this figure legend, the reader is referred to the web version of this article.)

previously reported, GM3 liposomes demonstrated high binding to CD169 Fc WT, while no binding to CD169 Fc mutant was observed (Fig. 1D). GM1 liposomes, similarly to control liposomes, did not bind to either of the recombinant CD169 Fc conjugates. To validate inclusion of ganglioside GM1 into the nanoparticle bilayer, we performed a lectin ELISA with peanut agglutinin (PNA), which specifically binds terminal β1,3-linked galactose [35]. As expected, only GM1 liposomes containing such structure bound to PNA, while control and GM3 liposomes did not (Fig. 1E).

Next, we evaluated the binding of liposomes to cell-surface expressed CD169 using a CD169-expressing CHO cell line transfected with CD169 WT or R97A mutant CD169 (Fig. 1F). CHO CD169 WT cells displayed very high DiD levels after incubation with GM3 liposomes in comparison to control and GM1 liposomes. In contrast, CHO CD169 R97A mutant cells did not take up GM3 liposomes. Accordingly, antibody-mediated blocking of the CD169 receptor largely diminished GM3 liposome capture.

Subsequently, we analyzed liposome binding and uptake by splenocytes *ex vivo*. While CD169 is highly expressed on CD169$^+$ macrophages, F4/80$^+$ red pulp macrophages display low expression of the receptor (Fig. S1). As expected, when we compared liposome binding at 4 °C and uptake at 37 °C, we observed an evident increase in liposome uptake at 37 °C (Fig. 2A and gating strategy in Fig. S2). This effect was most pronounced with GM3 liposomes as illustrated by increase in geometric mean fluorescence intensity (gMFI) of DiD, but we also observed some uptake of GM1 liposomes. *Ex vivo* CD169$^+$ macrophages sequestered extremely high levels of GM3 and significant lower levels of GM1 and control liposomes. Red pulp F4/80$^+$ macrophages and especially cDC1 capture much lower amounts of GM3 liposomes when compared to CD169$^+$ macrophages. Antibody-mediated blocking of the CD169 receptor (data not shown) and use of splenocytes isolated from mice expressing the W2QR97A mutant CD169 receptor (referred to as CD169 mutant) prevented uptake of GM3 liposomes by CD169$^+$ macrophages as well as by F4/80$^+$ red pulp macrophages and cDC1 (Fig. 2B and Fig. S3A). In contrast, other cell populations including cDC2, B cells, monocytes, T cells and NK cells displayed no liposome binding (data not shown).

In summary, these results clearly show that *in vitro* GM3 liposomes bind selectively to CD169 receptors, preferentially expressed by CD169$^+$ macrophages, whereas GM1 and control liposomes bind much lower or not to CD169$^+$ expressing cells.

3.2. Uptake of GM3 liposomes by CD169$^+$ macrophages in vivo is mediated by CD169

To determine whether GM3 liposomes are taken up by splenic CD169$^+$ macrophages *in vivo*, we i.v. administered control and ganglioside liposomes together with an adjuvant (anti-CD40/poly(I:C)) into WT and CD169 mutant animals (Fig. 3 and Fig. S3B). At 2 h post injection (p.i.), GM3 liposomes were predominantly sequestered by CD169$^+$ macrophages and to a substantially lesser extent by F4/80$^+$ red pulp macrophages, while hardly any liposome uptake was detected in cDC1. Contrary to the *in vitro* binding, CD169$^+$ macrophages also captured control and non-targeted GM1 liposomes *in vivo*, however the GM3 liposome uptake was more than three-fold higher (Fig. 3A). As expected, this increased uptake of GM3 liposomes by CD169$^+$ macrophages did not occur in CD169 mutant animals. Overall, these results indicate superior CD169-mediated uptake of GM3 liposomes as compared to non-CD169-mediated uptake of all liposomes. Liposome capture by cDC2, B cells, monocytes, T cells and NK cells was very low and appeared not to be dependent on the ganglioside modification of the liposome surface (Fig. S3B and data not shown).

Microscopic analysis of the spleen sections 2 h p.i. corroborated the flow cytometry data revealing clear co-localization of GM3 liposomes with CD169$^+$ macrophages in the marginal zone and lower association of control and GM1 liposomes with this macrophage subset (Fig. 3B). Similar to the 2 h time point, at 16 h p.i. CD169$^+$ macrophages displayed the highest GM3 liposome uptake when compared to other cell types. Furthermore, GM3 liposome uptake was significantly higher compared to control and GM1 liposomes also at 16 h p.i. (Fig. S3C).

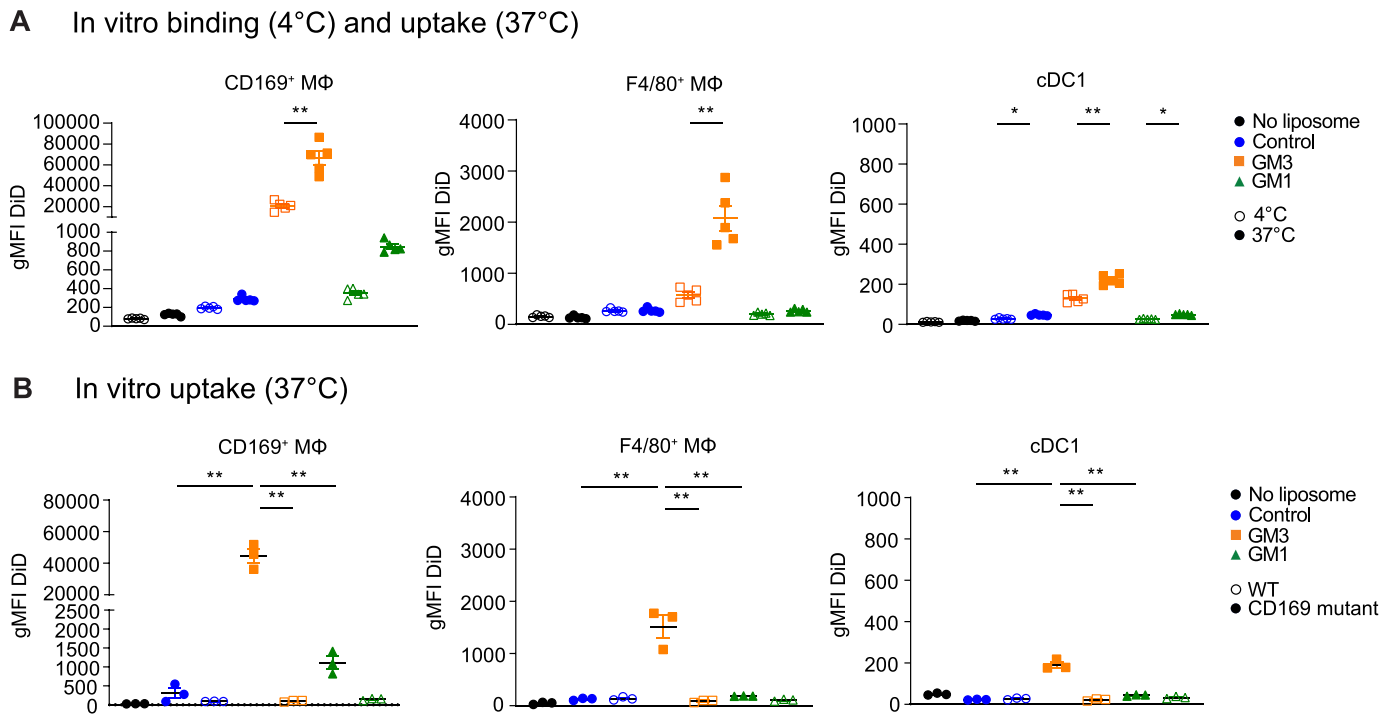

Fig. 2. GM3 liposomes are taken up by CD169$^+$ macrophages in a CD169-dependent manner *in vitro*. A. *In vitro* binding (4 °C) and uptake (37 °C) of liposomes to splenocytes determined by flow cytometry. B. *In vitro* uptake (37 °C) of liposomes by WT and CD169 mutant splenocytes determined by flow cytometry. The graphs show quantification of DiD gMFI. The data are from one experiment (A, $n = 5$) and from one experiment representative of three (B, $n = 3$). Each symbol represents one mouse. Error bars indicate mean ± SEM. *$p < 0.05$, **$p < 0.01$ (one-way ANOVA with Bonferroni's multiple comparison test).

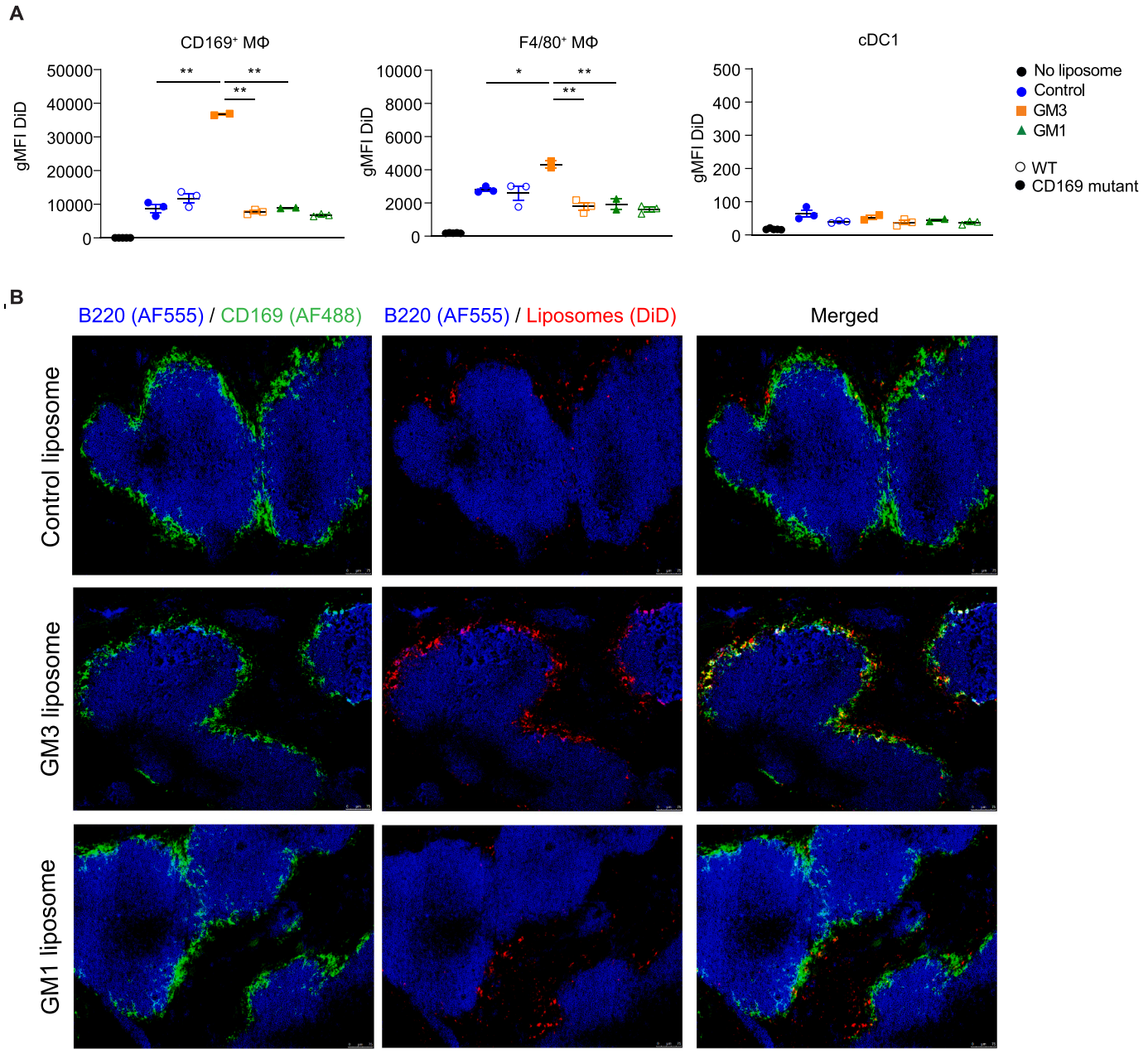

Fig. 3. GM3 liposomes are taken up by CD169$^+$ macrophages in a CD169-dependent manner *in vivo*. A-B WT and CD169 W2QR97A mutant (CD169 mutant) mice were injected i.v. with 70 nmoles liposomes (OVA 4 mg/ml) in the presence of adjuvant (25 μg anti-CD40 and 25 μg poly(I:C)). Uptake of liposomes in the spleen determined 2 h p.i. by flow cytometry (A) and microscopy (B). The graphs show quantification of DiD gMFI. The data are representative of two experiments ($n = 3$). Each symbol represents one mouse. Error bars indicate mean ± SEM. *$p < 0.05$, **$p < 0.01$ (one-way ANOVA with Bonferroni's multiple comparison test).

Taken together, these data demonstrate that CD169$^+$ macrophages efficiently capture liposomes *in vivo* and that the incorporation of GM3 significantly further enhances liposome uptake in a CD169-dependent fashion.

3.3. GM3 liposomes elicit superior immune responses in the presence of adjuvant

Next, we investigated the immunostimulatory capacity of the liposomes. To this end, WT animals were injected i.v. with OVA-containing GM3, non-targeting GM1 and control liposomes in the presence of a potent adjuvant combination, anti-CD40 and poly(I:C). Antigen-specific T cell and B cell responses in the spleen were determined 7 days after immunization. The magnitude of OVA-specific CD8$^+$ and CD4$^+$ T cell activation was measured with H-2K^b-SIINFEKL tetramer staining and intracellular IFNγ staining upon *ex vivo* re-challenge with cognate peptides. Additionally, we evaluated the OVA-specific germinal center B cell response and OVA-specific antibody titers. The flow cytometry analysis of tetramer staining revealed significantly higher frequencies of OVA-specific CD8$^+$ T cells in GM3 liposome-treated animals as compared to mice immunized with GM1 and control liposomes (Fig. 4A and gating strategy in Fig. S4). We observed a similar trend in the percentages of OVA-specific IFNγ producing CD8$^+$ and CD4$^+$ T cells, although this effect appeared not significant (Fig. 4A-B). In addition, significantly higher numbers of OVA$^+$ germinal center B cells were induced by immunization with GM3 and GM1 liposomes, when compared to control liposomes (Fig. 4C). Accordingly, we measured highest anti-OVA Ig titers in the serum of GM3 liposome-immunized mice (Fig. 4C and S5).

Immunization with OVA-containing control and ganglioside liposomes in the absence of the adjuvant revealed negligible induction of

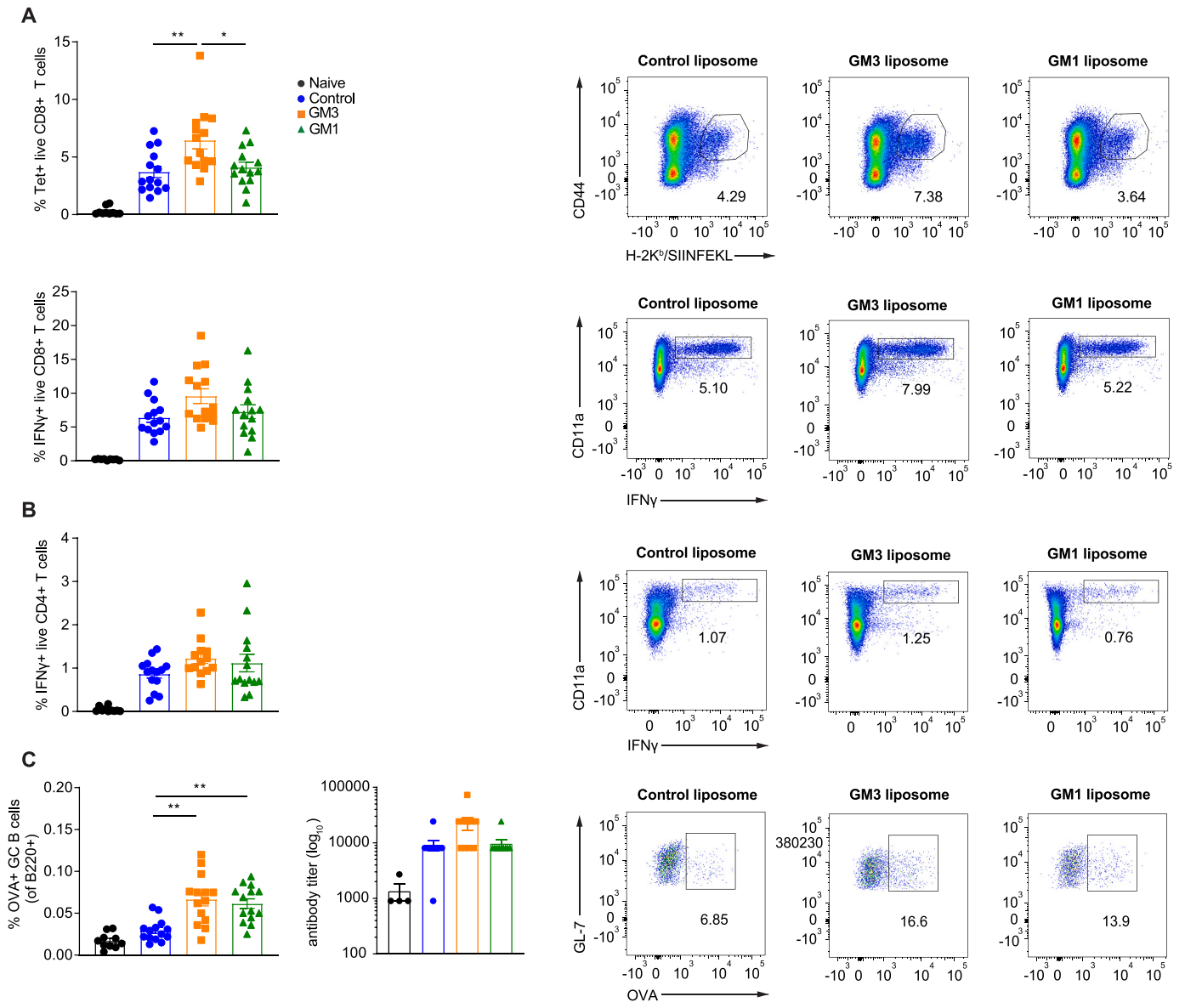

Fig. 4. GM3 liposomes elicit robust immune responses upon co-administration with adjuvant. A-C WT mice were injected i.v. with 93 nmoles liposomes (OVA 1 mg/ml) in the presence of adjuvant (25 μg anti-CD40 and 25 μg poly(I:C)) and the immune responses in the spleen were determined on day 7 p.i. by flow cytometry. A. Percentage of H-2K^b-SIINFEKL-tetramer$^+$ CD8$^+$ T cells and percentage of OVA-specific IFNγ-producing CD8$^+$ T cells. B. Percentage of OVA-specific IFNγ-producing CD4$^+$ T cells after *in vitro* re-challenge. C. Percentage of OVA-specific germinal center B cells (left) and serum titer of OVA-specific total Ig determined by ELISA (right). The data are from three experiments combined, $n = 14$ (left) and two experiments combined, $n = 10$ (right). Each symbol represents one mouse Error bars indicate mean ± SEM. *$p < 0.05$, **$p < 0.01$ (one-way ANOVA with Bonferroni's multiple comparison test).

OVA-specific T and B cell immunity (data not shown). This observation is in line with multiple cancer vaccination studies that demonstrate the necessity of adjuvant for immune activation [36–38]. Having demonstrated the importance of adjuvant in our vaccination platform, we next assessed the impact of liposomal antigen encapsulation on its immunogenicity. To address this, we immunized mice with GM3 and control OVA-containing liposomes or different doses of soluble OVA in the presence of adjuvant and evaluated immune activation on day 7 p.i. (Fig. S6). Liposomal-encapsulated OVA, equivalent to 0,2 μg of protein, proved to be more potent than 10 μg soluble OVA as illustrated by significantly higher frequency of antigen-specific T and B cells.

Collectively, these data indicate superior capacity of GM3 liposomes over non-targeted GM1 and control liposomes to stimulate effector T and B cell responses in the presence of adjuvant.

3.4. Liposomes delay tumor outgrowth, reduce tumor burden and improve survival in B16-OVA tumor model

Having demonstrated potent immune-activating capacity of the GM3 liposomes in naïve mice, we hypothesized that these nanoparticles show efficacy in a tumor setting. To test this idea, WT mice were injected subcutaneously into the flank with 3×10^5 OVA-expressing B16 tumor cells and once palpable tumors had developed (day 9), the mice were immunized with a single dose of OVA-containing liposomes and anti-CD40/poly(I:C) adjuvant (Fig. 5 and S7). Tumor growth and survival were monitored for 39 days. Strikingly, already 7 days after a single vaccination we observed significant reduction of tumor burden and delayed tumor growth in all treatment groups that maintained until day 25 post tumor inoculation (Fig. 5A-B). The decrease of tumor burden coincided with pronounced expansion of SIINFEKL$^+$ CD8$^+$ T cells in the blood of liposome-treated mice (Fig. 5C). Observed CD8$^+$ T cell response

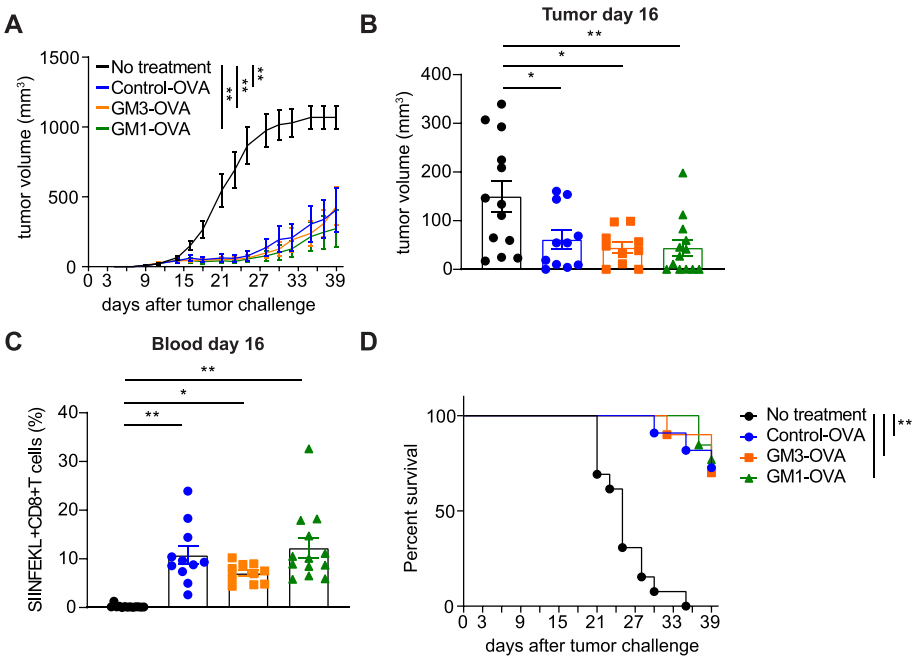

Fig. 5. Therapeutic vaccination with liposomes delays tumor growth and improves survival. A-D WT mice were s.c. inoculated in the flank with 3×10^5 B16-OVA tumor cells. On day 9 after tumor challenge, when tumors were palpable, the mice were injected i.v. with 93 nmoles liposomes (OVA 1 mg/ml) in presence of adjuvant (25 μg anti-CD40 and 25 μg poly (I:C)). A. Tumor growth curves determined by size measurements performed three times per week until day 39 using a caliper. Statistical comparison illustrated performed on day 39 after tumor challenge. B. Overall survival. C—D Mean tumor size (C) and percentage of H-2K^b-SIINFEKL-tetramer$^+$ CD8$^+$ T cells in blood (D) determined 7 days after immunization, on day 16 after tumor challenge. The data are from one experiment with no treatment, $n = 13$; control-OVA, $n = 11$; GM3-OVA, $n = 10$; GM1-OVA $n = 13$. Each symbol represents one mouse. Error bars indicate mean ± SEM. *$p < 0.05$, **$p < 0.01$ (one-way ANOVA with Bonferroni's multiple comparison test).

was of similar magnitude in all treatment groups, which correlates with the similar potency in tumor growth inhibition. Finally, tumor-bearing mice immunized with our OVA-containing liposomes exhibited significantly improved survival (Fig. 5D). These data clearly demonstrate the anti-tumor capacity of here evaluated liposome-based vaccine upon systemic administration.

3.5. CD169$^+$ macrophages bearing a functional CD169 receptor mediate generation of antigen-specific CD8$^+$ T cells after liposome vaccination

After examining the immune responses induced by liposomes in naïve and tumor-bearing mice, our next aim was to elucidate the underlying immune mechanism. Since CD169$^+$ macrophages were the main liposome-internalizing cell type *in vivo*, we first determined the importance of this macrophage subset in the liposome-mediated immune activation. To address this, we made use of the CD169-DTR mouse model that allows for selective depletion of CD169-expressing cells upon diphtheria toxin (DT) administration. Microscopic and flow cytometry analysis of the spleen tissue 48 h post DT injection confirmed successful elimination of CD169$^+$ cells leaving other cells unaffected (Fig. S8). Upon immunization with control and ganglioside liposomes co-injected with adjuvant, a significant decrease in the generation of OVA-specific CD8$^+$ T cells was detected when CD169$^+$ macrophages were depleted as detected by H-2K^b/SIINFEKL tetramer binding as well as OVA-specific IFNγ production (Fig. 6A). Interestingly, this was observed for all liposome types. Surprisingly, CD4$^+$ T cell and B cell immunity appeared not to be influenced by the absence of CD169$^+$ macrophages (Fig. 6B-C).

Since GM3 liposomes were sequestered by CD169$^+$ macrophages in a CD169-dependent fashion (Fig. 3), we hypothesized a role for CD169 in GM3 liposome-induced immunity. We immunized WT and CD169 mutant animals with OVA-containing control and ganglioside liposomes in the presence of adjuvant (Fig. 6D-E). CD169 mutant mice contained comparable numbers of CD169$^+$ macrophages and DCs compared to WT animals (Fig. S1). Upon i.v. administration of GM3 liposomes, WT mice exhibited significantly higher OVA-specific CD8$^+$ and CD4$^+$ T cell responses compared to CD169 mutant mice, as illustrated by intracellular IFNγ staining and tetramer staining (Fig. 6D). Apparently, the decrease in uptake of GM3 liposomes by mutant CD169$^+$ macrophages is directly translated into lower T cell responses. A similar trend, although not significant, was observed in animals immunized with control and GM1 liposomes. We have previously demonstrated a role for CD169 in the collaboration between CD169$^+$ macrophages and Batf3-dependent cDC1s after antigen-antibody targeting [12]. The results obtained here suggest that a CD169-mediated interaction may also play a minor role for T cell responses induced by control and GM1 liposomes that are taken up by CD169$^+$ macrophages in a CD169-independent manner.

Finally, when we examined OVA-specific germinal center B cell responses triggered by GM3 liposomes, we detected significantly diminished numbers of OVA$^+$ germinal center B cells in the mice bearing a mutated version of CD169 receptor, in comparison to WT animals (Fig. 6F). Although total anti-OVA Ig responses were not affected at this early time point, this finding suggests that CD169-mediated antigen uptake by CD169$^+$ macrophages also promotes germinal center B cell immunity.

In conclusion, together these data demonstrate that CD169$^+$ macrophages are essential for CD8$^+$ T cell priming after liposomal vaccination and that a functional CD169-receptor is necessary for GM3 liposome-mediated enhanced CD8$^+$ and CD4$^+$ T cell as well as germinal center B cell immune responses.

3.6. cDC1 are essential for CD8$^+$ T cell responses induced by GM3 liposomes

The previous experiments demonstrated an important role for CD169$^+$ macrophages in CD8$^+$ T cell priming. CD169$^+$ macrophages could be directly involved in antigen presentation to and activation of CD8$^+$ T cells or alternatively could collaborate with cDC1 for CD8$^+$ T cell priming as previously observed in antibody-mediated antigen targeting [12]. To evaluate the role of cDC1 in liposome-induced immunity, we measured immune responses in WT and Batf3KO mice i.v. immunized with OVA-containing control and ganglioside liposomes in presence of the adjuvant. OVA-specific CD8$^+$ T cell responses were inhibited to background levels in Batf3KO animals compared to WT animals for GM3, GM1 and control liposomes, as illustrated by tetramer and intracellular IFNγ staining (Fig. 7A). While the absence of cDC1 during liposome immunization also negatively affected the generation of IFNγ producing CD4$^+$ T cells (Fig. 7B), this was not the case for the OVA-specific germinal center B cell population and antibody titers (Fig. 7C).

In conclusion, these results confirm the crucial role of Batf3-

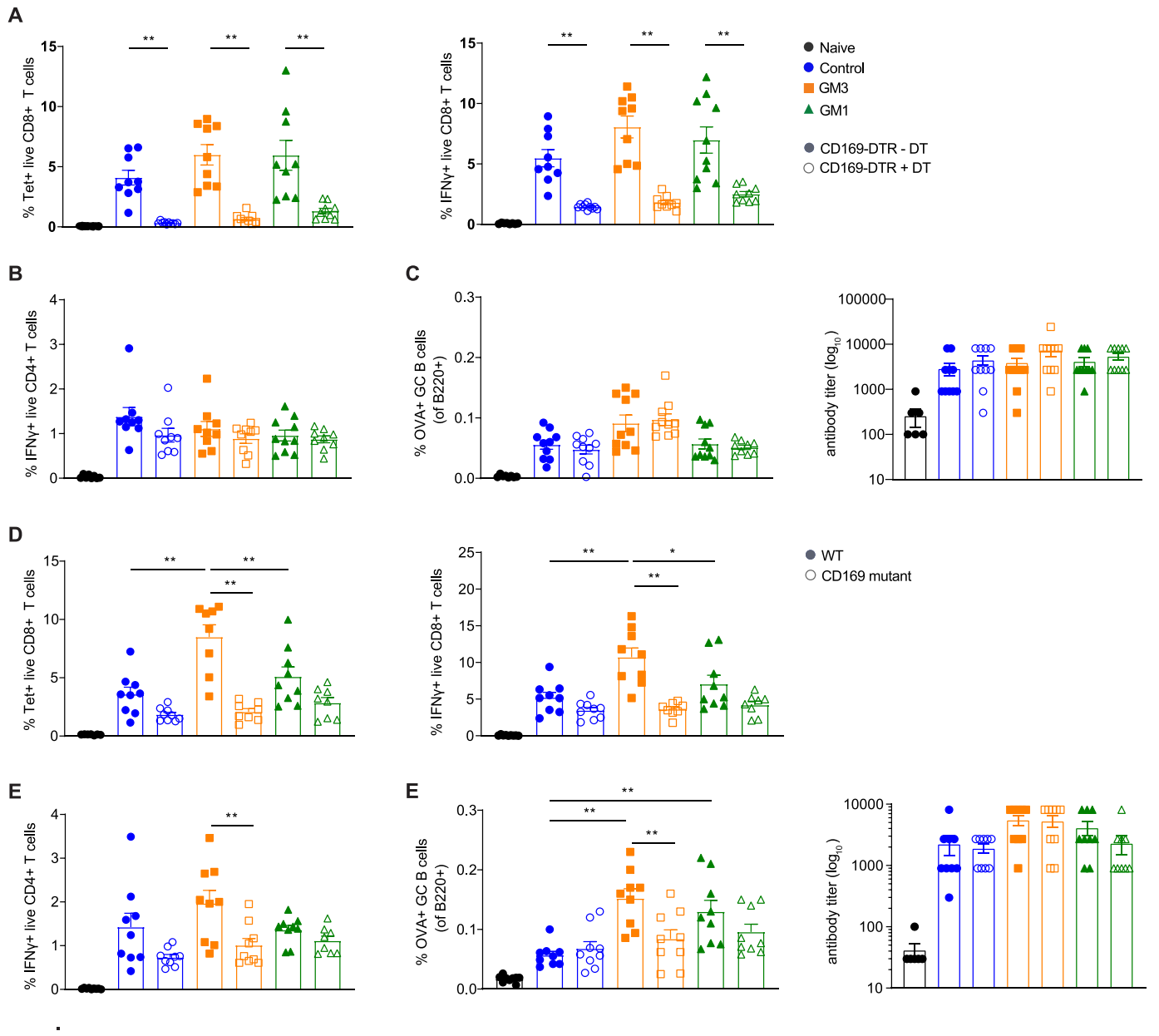

Fig. 6. CD169$^+$ macrophages expressing a functional CD169 receptor orchestrate GM3 liposome-induced CD8$^+$ T cell activation. A-C CD169-DTR mice were injected or not i.v. with 40 ng/g mouse of diphtheria toxin (DT) on day 0 and with 93 nmoles liposomes (OVA 1 mg/ml) in presence of adjuvant (25 μg anti-CD40 and 25 μg poly(I:C)) on day 2. The immune responses in the spleen were determined on day 7 p.i. with liposomes by flow cytometry. D—F WT and W2QR97A mutant (CD169 mutant) mice were injected i.v. with 93 nmoles liposomes (OVA 1 mg/ml) in presence of adjuvant (25 μg anti-CD40 and 25 μg poly(I:C)) and the immune responses in the spleen were determined on day 7 p.i.. by flow cytometry. A,D Percentage of H-2K^b-SIINFEKL-tetramer$^+$ CD8$^+$ T cells and percentage of OVA-specific IFNγ-producing CD8$^+$ T cells. B,E Percentage of OVA-specific IFNγ-producing CD4$^+$ T cells after *in vitro* re-challenge. C,F Percentage of OVA-specific germinal center B cells (left) and serum titer of OVA-specific total Ig determined by ELISA (right). The data are from two experiments combined, $n = 10$ (A-C) and $n = 9$ (D—F). Each symbol represents one mouse. Error bars indicate mean ± SEM. $^*p < 0.05$, $^{**}p < 0.01$ (one-way ANOVA with Bonferroni's multiple comparison test).

dependent cross-presenting DCs for generation of potent CD8$^+$ T cell responses triggered not only by GM3 liposomes, but also by control and non-targeted GM1 liposomes.

4. Discussion

The enormous progress in cancer immunotherapy in the last decade has emphasized the importance of a strong anti-tumor CD8$^+$ T cell response to achieve tumor eradication [39]. Current challenges in the field focus on the induction or the improvement of CD8$^+$ T cell activation in checkpoint inhibitor-treated cancer patients by combining it with a synergistic strategy, such as cancer vaccination. Although DCs are favored targets for antigen delivery to induce antigen-specific immunity [9,40,41], CD169$^+$ macrophages have emerged as an attractive alternative to antigen presenting cells for antigen targeting. We and others have previously shown that CD169$^+$ macrophages efficiently capture pathogens and antibody-conjugated antigens from lymph fluid and blood and stimulate robust CD8$^+$ T cell responses in collaboration with cross-presenting DC1s [11–14,16,42].

Here we demonstrate for the first time that these two cell types are also responsible for CD8$^+$ T cell priming after liposomal vaccination. We show that CD169$^+$ macrophages not only efficiently take up CD169-targeted GM3-containing liposomes, but also non-targeted liposomes. Our studies further indicate that CD169$^+$ cannot activate CD8$^+$ T cell

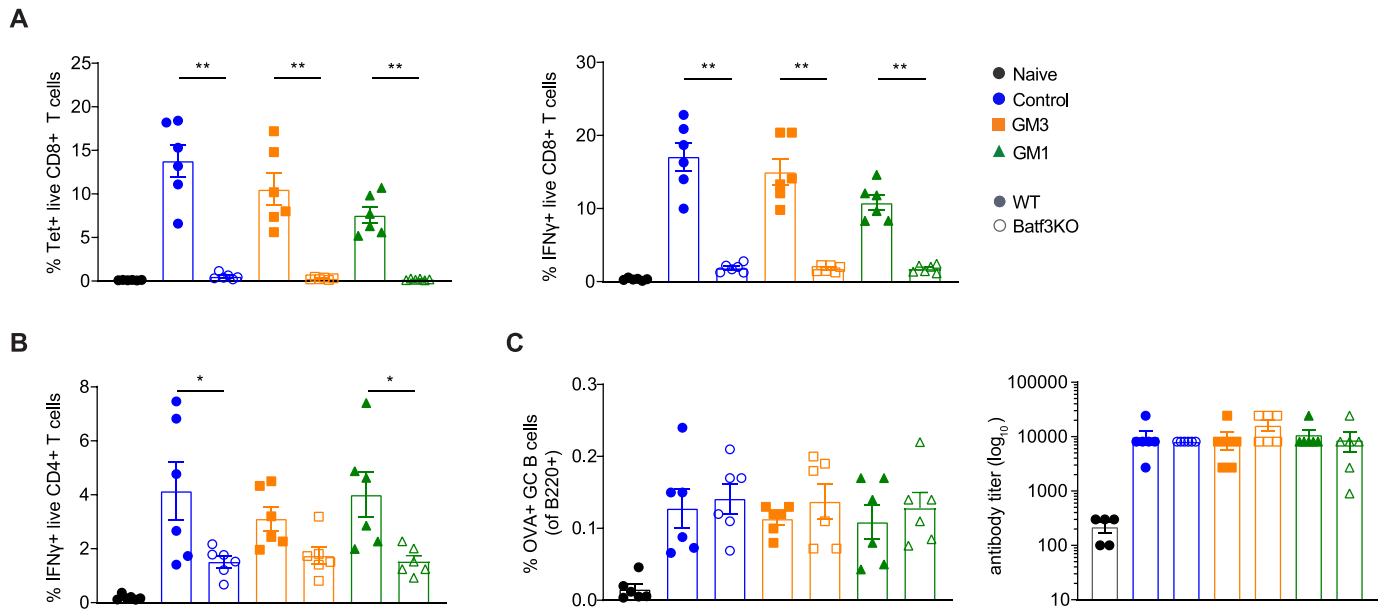

Fig. 7. Cross-presenting DCs orchestrate liposome-induced CD8$^+$ T cell activation. WT and Batf3KO animals were injected i.v. with 200 nmoles liposomes (OVA 4 mg/ml) in presence of adjuvant (25 μg anti-CD40 and 25 μg poly(I:C)) and the immune responses in the spleen were determined on day 7 p.i.. by flow cytometry. A. Percentage of H-2K^b-SIINFEKL-tetramer$^+$ CD8$^+$ T cells and percentage of OVA-specific IFNγ-producing CD8$^+$ T cells. B. Percentage of OVA-specific IFNγ-producing CD4$^+$ T cells after *in vitro* re-challenge. C. Percentage of OVA-specific germinal center B cells (left) and serum titer of OVA-specific total Ig determined by ELISA (right). The data are from two experiments combined, $n = 6$. Each symbol represents one mouse. Error bars indicate mean ± SEM. $^*p < 0.05$, $^{**}p < 0.01$ (one-way ANOVA with Bonferroni's multiple comparison test).

responses by themselves, but require the presence of Batf3-dependent cDC1s for CD8$^+$ T cell priming. Since we did not investigate the mechanism of this mutual requirement for induction of CD8$^+$ T cells, we can only speculate about the processes that could mediate such interdependency. One possibility is that CD169$^+$ macrophages, that are apparently specialized in liposome uptake from the blood, efficiently transfer captured liposomes to cDC1s, which are present in close proximity due to interaction with CD169 receptor *via* sialic acids [12]. Nevertheless, we did not detect clear changes in cDC1-associated DiD fluorescence in WT animals at 16 h p.i. (from 2 h), neither in DT-treated CD169-DTR mice (data not shown) nor in CD169 mutant mice, which would support or disprove the antigen transfer hypothesis. However, care must be taken when interpreting these findings as DiD is located in the bilayer and thus may follow different routes than the encapsulated protein antigen upon liposome disintegration. An alternative explanation for the requirement of both CD169$^+$ macrophages and cDC1 could be that CD169$^+$ macrophages enhance the capacity of cDC1s to cross-present and subsequently activate CD8$^+$ T cells *e.g. via* the production of type I interferons [43–46]. Future studies are necessary to elucidate the exact mechanism(s) underlying cooperation between CD169$^+$ macrophages and cDC1s after liposomal vaccination.

Another surprising result from our studies is that although CD169$^+$ are essential for CD8$^+$ T cell priming, these cells appeared not to be necessary for activation of B cell immunity upon liposomal challenge. In a number of seminal studies, lymph node CD169$^+$ macrophages were shown to present antigen to B cells and we previously reported strong B cell responses after antibody-mediated antigen targeting to CD169$^+$ macrophages, which were eliminated after treatment with clodronate liposomes [47–50]. In line with this, here we observed induction of antigen-specific B cells after enhanced targeting to CD169$^+$ macrophages using GM3 liposomes (Fig. 4) but, unexpectedly, B cell responses remained unaffected in CD169-DTR mouse model (Fig. 6). It has to be noted that the CD169 depletion experiments are difficult to interpret as in the absence of CD169$^+$ macrophages we detected higher uptake of liposomes by all other cell types (data not shown). This suggests that the clearance rate of liposomes is significantly decreased in the absence of CD169$^+$ macrophages. Furthermore, the removal of CD169$^+$ macrophages, which are located on top of the B cell follicles, may dramatically change the localization of liposomes and subsequent uptake patterns, and thus precludes clear comparison between both conditions. Aside of these considerations, another mechanism of B cell activation that is independent of CD169$^+$ macrophages could well be operational in our liposomal vaccination strategy. Marginal zone B cells are known to transport immune complexes into B cell follicles [51–53] and a complement-IgM-dependent pathway has also been described for the transport of PEGylated liposomes by marginal zone B cells [54,55]. Therefore, a complement-dependent B cell activation that is independent of CD169$^+$ macrophages may be involved after liposomal vaccination.

Systemically administered nanoparticles interact with plasma proteins resulting in a protein layer adsorbed on the surface of nanoparticles, also known as the protein corona (reviewed by [56–58]). Although nanoparticles carrying a positive charge exhibit an increased association with serum proteins, a protein corona is also formed on anionic nanoparticles. Since the protein corona has been found to modulate nanoparticle characteristics and behavior *in vivo*, it might also affect here investigated liposomes. Opsonization and complement activation could potentially be involved in the non-CD169 receptor-mediated uptake of control and GM1 liposomes by CD169$^+$ macrophages, observed *in vivo*. Complement factors and various plasma proteins enriched in serum affect liposome internalization *via* opsonin receptor-dependent mechanism involving complement system and Fc receptors [59]. In fact, anionic liposomes are potent stimulators of complement system and complement component C1q and scavenger receptors have been previously implicated in the sequestration of intravenously injected anionic nanoparticles by antigen presenting cells [60–62]. Thus, complement-mediated mechanisms could potentially be responsible for the *in vivo* uptake of anionic liposomes by macrophages and their capacity to elicit immune responses in the presence of adjuvant.

One of the primary aims of this study was to investigate the effect of specific antigen targeting to CD169$^+$ macrophages using GM3 liposomes on immune responses and tumor reactivity. Our data clearly shows the

importance of a functional CD169 receptor for enhanced GM3 liposome uptake by these macrophages *in vitro* and *in vivo* as well as augmented $CD8^+$ T cell and B cell responses. While we observed a strong inhibition of tumor outgrowth in all vaccinated mice, we did not detect enhanced tumor reactivity of GM3 liposomes when compared to control or GM1 liposomes. In the present study we systemically co-injected liposomes with a very potent adjuvant, which may augment immune response induced by less efficient targeted liposomes *i.e.* control and GM1 liposomes, possibly compromising the potential efficacy of CD169 targeting. Future studies in which we will combine antigen and adjuvant in one $CD169^+$ macrophage-targeting nanoparticle may exhibit better efficacy. Recently, Edgar, Kawasaki [63] investigated CD169-targeted nanoparticles bearing a synthetic high affinity ligand for CD169. The authors showed that selective liposomal delivery of both the antigen and toll-like receptor 7 agonist (TLR7 agonist) to $CD169^+$ macrophages drove efficient $CD8^+$ T cell expansion. This suggests that incorporation of TLR7 ligand may further enhance the activity of GM3 liposomes. Ganglioside GM3 offers an important advantage over a synthetic molecule as CD169 ligand. Being widely expressed in the body, GM3 will not elicit an immune response, in contrast to foreign molecules incorporated in liposomes such as PEG, which upon repeated administration causes adverse hypersensitivity reactions [64].

Our results demonstrating enhanced targeting of GM3 liposomes to $CD169^+$ macrophages *in vivo* are in line with human *in vitro* studies using GM3-containing nanoparticles, which reported specific binding to human CD169-expressing macrophages and monocyte-derived DCs [20,22,65]. We recently showed that several ganglioside-containing liposomes can bind to *ex vivo* human splenic macrophages as well as blood-derived Axl^+ Siglec-6-expressing DCs and subsequently activate $CD8^+$ T cells [66]. Furthermore, here presented findings verify the selectivity of GM3 for CD169/Siglec-1, as we did not observe binding to other Siglec receptors expressed by various other cell types such as DCs, B cells and NK cells [19]. Multiple studies have shown that marginal zone $CD169^+$ macrophages are the predominant cell type to capture viruses including HIV, MLV and Ebola additionally revealing gangliosides as mediators of the binding to CD169 [46,67–71]. Similarly, GM3 liposomes can be regarded as virus-like nanoparticles that appear to selectively bind to CD169 receptor.

Currently, a multitude of liposome-based vaccine vectors that display different characteristics are being tested as anti-cancer therapeutics [8,72]. In fact, negatively charged RNA-lipoplexes have been shown to successfully target splenic macrophages and DCs when administered i.v. resulting in potent (anti-cancer) CTL responses in mice and in humans [73–75]. Importantly, our studies demonstrate the crucial role of $CD169^+$ macrophages and cross-presenting cDC1s for the immune responses induced by liposomes. In addition, we show that the addition of GM3 to anionic liposomes significantly enhances antigen delivery to splenic $CD169^+$ macrophages and subsequent induction of $CD8^+$ T cell immunity. Further elucidation of the cellular interactions in lymphoid organs after vaccine uptake will expand our knowledge on the immunogenicity of nanoparticle-based antigen targeting platforms and will guide optimal nanoparticle design for cancer vaccination.

Acknowledgements

This work was supported by grants from the Dutch Cancer Society (VU2016-10449) to JMMdH, by NWO ZonMW TOP 91218024 to JMMdH and GS, and from the Phospholipid Research Center (JDH-2020-082/1-1) to JMMdH and YvK. We thank the staff of Amsterdam UMC Animal Facility (location VUmc) for animal care, especially R. van der Laan. We acknowledge the Microscopy and Cytometry Core Facility (MCCF) at the Amsterdam UMC – Location VUmc for providing assistance with microscopy and cytometry.

Appendix A. Supplementary data

Supplementary data to this article can be found online at https://doi.org/10.1016/j.jconrel.2021.01.029.

References

[1] T.K. Kim, R.S. Herbst, L. Chen, Defining and understanding adaptive resistance in Cancer immunotherapy, Trends Immunol. 39 (8) (2018) 624–631.
[2] S.H. van der Burg, et al., Vaccines for established cancer: overcoming the challenges posed by immune evasion, Nat. Rev. Cancer 16 (4) (2016) 219–233.
[3] P.A. Ott, et al., Combination immunotherapy: a road map, J. Immunother. Cancer 5 (2017) 16.
[4] J.M. Collins, J.M. Redman, J.L. Gulley, Combining vaccines and immune checkpoint inhibitors to prime, expand, and facilitate effective tumor immunotherapy, Expert Rev. Vaccines 17 (8) (2018) 697–705.
[5] B.J. Coventry, Therapeutic vaccination immunomodulation: forming the basis of all cancer immunotherapy, Ther. Adv. Vaccin. Immunother. 7 (2019), p. 2515135519862234.
[6] A. Mougel, M. Terme, C. Tanchot, Therapeutic cancer vaccine and combinations with Antiangiogenic therapies and immune checkpoint blockade, Front. Immunol. 10 (2019) 467.
[7] J. Strauss, R.A. Madan, J.L. Gulley, Considerations for the combination of anticancer vaccines and immune checkpoint inhibitors, Expert. Opin. Biol. Ther. 16 (7) (2016) 895–901.
[8] R.E. Hollingsworth, K. Jansen, Turning the corner on therapeutic cancer vaccines, NPJ Vaccin. 4 (2019) 7.
[9] S.K. Wculek, et al., Dendritic cells in cancer immunology and immunotherapy, Nat. Rev. Immunol. 20 (1) (2019) 7–24.
[10] J.P. Bottcher, E.S.C. Reis, The role of type 1 conventional dendritic cells in cancer immunity, Trends Cancer 4 (11) (2018) 784–792.
[11] R. Backer, et al., Effective collaboration between marginal metallophilic macrophages and CD8+ dendritic cells in the generation of cytotoxic T cells, Proc. Natl. Acad. Sci. U. S. A. 107 (1) (2010) 216–221.
[12] D. van Dinther, et al., Functional CD169 on macrophages mediates interaction with dendritic cells for CD8(+) T cell cross-priming, Cell Rep. 22 (6) (2018) 1484–1495.
[13] D. van Dinther, et al., Comparison of protein and peptide targeting for the development of a CD169-based vaccination strategy against melanoma, Front. Immunol. 9 (2018) 1997.
[14] C.A. Bernhard, et al., CD169+ macrophages are sufficient for priming of CTLs with specificities left out by cross-priming dendritic cells, Proc. Natl. Acad. Sci. U. S. A. 112 (17) (2015) 5461–5466.
[15] K. Asano, et al., CD169-positive macrophages dominate antitumor immunity by crosspresenting dead cell-associated antigens, Immunity 34 (1) (2011) 85–95.
[16] J. Grabowska, et al., CD169(+) macrophages capture and dendritic cells instruct: the interplay of the gatekeeper and the general of the immune system, Front. Immunol. 9 (2018) 2472.
[17] D.A.P. Louie, S. Liao, Lymph node subcapsular sinus macrophages as the frontline of lymphatic immune defense, Front. Immunol. 10 (2019) 347.
[18] K. Asano, K. Kikuchi, M. Tanaka, CD169 macrophages regulate immune responses toward particulate materials in the circulating fluid, J. Biochem. 164 (2) (2018) 77–85.
[19] M.S. Macauley, P.R. Crocker, J.C. Paulson, Siglec-mediated regulation of immune cell function in disease, Nat. Rev. Immunol. 14 (10) (2014) 653–666.
[20] W.B. Puryear, et al., HIV-1 incorporation of host-cell-derived glycosphingolipid GM3 allows for capture by mature dendritic cells, Proc. Natl. Acad. Sci. U. S. A. 109 (19) (2012) 7475–7480.
[21] H. Akiyama, et al., Virus particle release from glycosphingolipid-enriched microdomains is essential for dendritic cell-mediated capture and transfer of HIV-1 and henipavirus, J. Virol. 88 (16) (2014) 8813–8825.
[22] N. Izquierdo-Useros, et al., Siglec-1 is a novel dendritic cell receptor that mediates HIV-1 trans-infection through recognition of viral membrane gangliosides, PLoS Biol. 10 (12) (2012), e1001448.
[23] B.E. Collins, et al., Binding specificities of the sialoadhesin family of I-type lectins. Sialic acid linkage and substructure requirements for binding of myelin-associated glycoprotein, Schwann cell myelin protein, and sialoadhesin, J. Biol. Chem. 272 (27) (1997) 16889–16895.
[24] Y. Hashimoto, et al., A streptavidin-based neoglycoprotein carrying more than 140 GT1b oligosaccharides: quantitative estimation of the binding specificity of murine sialoadhesin expressed on CHO cells, J. Biochem. 123 (3) (1998) 468–478.
[25] P.R. Crocker, et al., Purification and properties of sialoadhesin, a sialic acid-binding receptor of murine tissue macrophages, EMBO J. 10 (7) (1991) 1661–1669.
[26] M.D. Joshi, et al., Targeting tumor antigens to dendritic cells using particulate carriers, J. Control. Release 161 (1) (2012) 25–37.
[27] L.O. De Serrano, D.J. Burkhart, Liposomal vaccine formulations as prophylactic agents: design considerations for modern vaccines, J. Nanobiotechnol. 15 (1) (2017) 83.
[28] Z. Gu, et al., Liposome-based drug delivery systems in cancer immunotherapy, Pharmaceutics 12 (11) (2020).
[29] M. Klaas, et al., Sialoadhesin promotes rapid proinflammatory and type I IFN responses to a sialylated pathogen, *Campylobacter jejuni*, J. Immunol. 189 (5) (2012) 2414–2422.

[30] Y. Miyake, et al., Critical role of macrophages in the marginal zone in the suppression of immune responses to apoptotic cell-associated antigens, J. Clin. Invest. 117 (8) (2007) 2268–2278.
[31] M. Saito, et al., Diphtheria toxin receptor-mediated conditional and targeted cell ablation in transgenic mice, Nat. Biotechnol. 19 (8) (2001) 746–750.
[32] M.A. de Witte, et al., Targeting self-antigens through allogeneic TCR gene transfer, Blood 108 (3) (2006) 870–877.
[33] T.C. Albershardt, et al., Intratumoral immune activation with TLR4 agonist synergizes with effector T cells to eradicate established murine tumors, NPJ Vaccin. 5 (2020) 50.
[34] W.B. Puryear, et al., Interferon-inducible mechanism of dendritic cell-mediated HIV-1 dissemination is dependent on Siglec-1/CD169, PLoS Pathog. 9 (4) (2013), e1003291.
[35] Y. Ma, et al., Liposomal glyco-microarray for studying glycolipid-protein interactions, Anal. Bioanal. Chem. 404 (1) (2012) 51–58.
[36] I. Melero, et al., Therapeutic vaccines for cancer: an overview of clinical trials, Nat. Rev. Clin. Oncol. 11 (9) (2014) 509–524.
[37] C.J. Melief, et al., Therapeutic cancer vaccines, J. Clin. Invest. 125 (9) (2015) 3401–3412.
[38] W.W. Overwijk, Cancer vaccines in the era of checkpoint blockade: the magic is in the adjuvant, Curr. Opin. Immunol. 47 (2017) 103–109.
[39] D.C. Tscharke, et al., Sizing up the key determinants of the CD8(+) T cell response, Nat. Rev. Immunol. 15 (11) (2015) 705–716.
[40] K.F. Bol, et al., Dendritic cell-based immunotherapy: state of the art and beyond, Clin. Cancer Res. 22 (8) (2016) 1897–1906.
[41] K. Palucka, J. Banchereau, Dendritic-cell-based therapeutic cancer vaccines, Immunity 39 (1) (2013) 38–48.
[42] M. Habbeddine, et al., Receptor activator of NF-kappaB orchestrates activation of antiviral memory CD8 T cells in the spleen marginal zone, Cell Rep. 21 (9) (2017) 2515–2527.
[43] A. Le Bon, et al., Cross-priming of CD8+ T cells stimulated by virus-induced type I interferon, Nat. Immunol. 4 (10) (2003) 1009–1015.
[44] M.S. Diamond, et al., Type I interferon is selectively required by dendritic cells for immune rejection of tumors, J. Exp. Med. 208 (10) (2011) 1989–2003.
[45] M.B. Fuertes, et al., Host type I IFN signals are required for antitumor CD8+ T cell responses through CD8{alpha}+ dendritic cells, J. Exp. Med. 208 (10) (2011) 2005–2016.
[46] N. Shaabani, et al., CD169(+) macrophages regulate PD-L1 expression via type I interferon and thereby prevent severe immunopathology after LCMV infection, Cell Death Dis. 7 (11) (2016), e2446.
[47] H. Veninga, et al., Antigen targeting reveals splenic CD169+ macrophages as promoters of germinal center B-cell responses, Eur. J. Immunol. 45 (3) (2015) 747–757.
[48] T. Junt, et al., Subcapsular sinus macrophages in lymph nodes clear lymph-borne viruses and present them to antiviral B cells, Nature 450 (7166) (2007) 110–114.
[49] T.G. Phan, et al., Immune complex relay by subcapsular sinus macrophages and noncognate B cells drives antibody affinity maturation, Nat. Immunol. 10 (7) (2009) 786–793.
[50] T.G. Phan, et al., Subcapsular encounter and complement-dependent transport of immune complexes by lymph node B cells, Nat. Immunol. 8 (9) (2007) 992–1000.
[51] G. Cinamon, et al., Follicular shuttling of marginal zone B cells facilitates antigen transport, Nat. Immunol. 9 (1) (2008) 54–62.
[52] L. Zhang, et al., Marginal zone B cells transport IgG3-immune complexes to splenic follicles, J. Immunol. 193 (4) (2014) 1681–1689.
[53] A.R. Ferguson, M.E. Youd, R.B. Corley, Marginal zone B cells transport and deposit IgM-containing immune complexes onto follicular dendritic cells, Int. Immunol. 16 (10) (2004) 1411–1422.
[54] T. Shimizu, et al., Anti-PEG IgM and complement system are required for the association of second doses of PEGylated liposomes with splenic marginal zone B cells, Immunobiology 220 (10) (2015) 1151–1160.
[55] T. Shimizu, et al., A novel platform for Cancer vaccines: antigen-selective delivery to splenic marginal zone B cells via repeated injections of PEGylated liposomes, J. Immunol. 201 (10) (2018) 2969–2976.
[56] T. Lima, et al., Understanding the lipid and protein Corona formation on different sized polymeric nanoparticles, Sci. Rep. 10 (1) (2020) 1129.
[57] M. Bros, et al., The protein Corona as a confounding variable of nanoparticle-mediated targeted vaccine delivery, Front. Immunol. 9 (2018) 1760.
[58] D. Chen, et al., Protein Corona-enabled systemic delivery and targeting of nanoparticles, AAPS J. 22 (4) (2020) 83.
[59] J.A. Kamps, G.L. Scherphof, Receptor versus non-receptor mediated clearance of liposomes, Adv. Drug Deliv. Rev. 32 (1–2) (1998) 81–97.
[60] J. Szebeni, The interaction of liposomes with the complement system, Crit. Rev. Ther. Drug Carrier Syst. 15 (1) (1998) 57–88.
[61] N. Benne, et al., Anionic 1,2-distearoyl-sn-glycero-3-phosphoglycerol (DSPG) liposomes induce antigen-specific regulatory T cells and prevent atherosclerosis in mice, J. Control. Release 291 (2018) 135–146.
[62] A. Chonn, P.R. Cullis, D.V. Devine, The role of surface charge in the activation of the classical and alternative pathways of complement by liposomes, J. Immunol. 146 (12) (1991) 4234–4241.
[63] L.J. Edgar, et al., Targeted delivery of antigen to activated CD169(+) macrophages induces Bias for expansion of CD8(+) T cells, Cell Chem. Biol. 26 (1) (2019) 131–136 (e4).
[64] M. Mohamed, et al., PEGylated liposomes: immunological responses, Sci. Technol. Adv. Mater. 20 (1) (2019) 710–724.
[65] X. Yu, et al., Glycosphingolipid-functionalized nanoparticles recapitulate CD169-dependent HIV-1 uptake and trafficking in dendritic cells, Nat. Commun. 5 (2014) 4136.
[66] A.J. Affandi, et al., Selective tumor antigen vaccine delivery to human CD169(+) antigen-presenting cells using ganglioside-liposomes, Proc. Natl. Acad. Sci. U. S. A. 117 (44) (2020) 27528–27539.
[67] X. Sewald, et al., Retroviruses use CD169-mediated trans-infection of permissive lymphocytes to establish infection, Science 350 (6260) (2015) 563–567.
[68] D. Perez-Zsolt, et al., Anti-Siglec-1 antibodies block Ebola viral uptake and decrease cytoplasmic viral entry, Nat. Microbiol. 4 (9) (2019) 1558–1570.
[69] N. Honke, et al., Enforced viral replication activates adaptive immunity and is essential for the control of a cytopathic virus, Nat. Immunol. 13 (1) (2012) 51–57.
[70] P.V. Shinde, et al., Tumor necrosis factor-mediated survival of CD169(+) cells promotes immune activation during vesicular stomatitis virus infection, J. Virol. (2018) 92(3).
[71] V. Duhan, et al., Virus-specific antibodies allow viral replication in the marginal zone, thereby promoting CD8(+) T-cell priming and viral control, Sci. Rep. 6 (2016) 19191.
[72] U. Bulbake, et al., Liposomal formulations in clinical use: an updated review, Pharmaceutics 9 (2) (2017).
[73] K. Broos, et al., Particle-mediated intravenous delivery of antigen mRNA results in strong antigen-specific T-cell responses despite the induction of type I interferon, Mol. Ther. Nucleic Acids 5 (6) (2016), e326.
[74] L.M. Kranz, et al., Systemic RNA delivery to dendritic cells exploits antiviral defence for cancer immunotherapy, Nature 534 (7607) (2016) 396–401.
[75] U. Sahin, et al., An RNA vaccine drives immunity in checkpoint-inhibitor-treated melanoma, Nature 585 (7823) (2020) 107–112.
[76] M.A. Boks, MPLA incorporation into DC-targeting glycoliposomes favours anti-tumour T cell responses, Journal of Controlled Release (2015), https://doi.org/10.1016/j.jconrel.2015.06.033.